Available online at www.sciencedirect.com
ScienceDirect
Journal of Solid State Chemistry 181 (2008) 822–827
JOURNAL OF SOLID STATE CHEMISTRY
www.elsevier.com/locate/jssc

Controlled modification of multiwalled carbon nanotubes with Zno nanostructures

Xiuying Wang, Baiying Xia, Xingfu Zhu, Jiesheng Chen, Shilun Qiu, Jixue Li*

State Key Laboratory of Inorganic Synthesis and Preparative Chemistry, College of Chemistry, Jilin University, Changchun 130012, PR China

Received 9 September 2007; received in revised form 30 December 2007; accepted 6 January 2008
Available online 10 January 2008

Abstract

Multiwalled carbon nanotubes (MWNTs) have been successfully modified with ZnO nanostructures by zinc–ammonitum complex ion covalently attached to the MWNTs through the C–N bonds. Flower-like ZnO on the tips of MWNTs and ZnO nanoparticles on the surface of MWNTs have been obtained, respectively, via adjusting the reaction time. The modified MWNTs have been characterized with X-ray diffraction, scanning electron and transmission electron microscopy. A growth mechanism has been proposed in which the soaking time plays a key role in controlling the size, morphology, and site of ZnO nanostructures. Photoluminescence properties of the as-synthesized products have also been investigated.

Keywords: Carbon nanotubes; Flower-like; Heterojunctions; Zinc oxide; Composites

1. Introduction

Carbon nanotube (CNT), exhibiting novel structure and unique properties, has been paid a great deal of attention since it was discovered [1]. It has been indicated that the CNT properties can be dramatically influenced by the surface modification with organic, inorganic and biological species [2–7]. It is therefore that the researches on CNT are focusing on the surface modification, and many metal oxides and sulfides such as TiO_2, SnO_2, ZnS and CdS [8–11], have been successfully used to modify CNT. Among a series of semiconductors, zinc oxide with a direct band gap (3.37 eV) and a relatively high exciton binding energy (~60 meV) is particularly attractive and its potentials as room-temperature UV lasers, light-emitting diodes and sensors have been investigated for several decades [12–15]. Recently, studies indicate that CNT/ZnO composite could possess unique properties which are different from alone CNT and ZnO. Up to now, various methods, such as chemical vapor deposition (CVD), plasma-assisted sputter and microwave irradiation heating, have been carried out to modify CNT with ZnO [16–18]. However, achieving control over the size and morphology of the CNT/ZnO composite is still challenging. Exclusively tip-decorated CNT/ZnO heterojunction arrays have been obtained by a water-assisted chemical vapor deposition of carbon on a zinc foil [16], and beading of ZnO nanoparticles on the sidewalls of multiwalled CNTs (MWNTs) has also been achieved [17], but by what means control over the morphology, size and site of ZnO structures attaching on the CNT remains an open question. In addition, the large-scale industrial preparation of CNT/ZnO composites by a controlled methodology is still difficult. In comparison with traditional vapor deposition approaches, wet-chemical methods can provide a better opportunity for control over the size and morphology of basic ZnO nanometer-scale units for building CNT/ZnO composites. More importantly, the route allows for an easier realization of the industrial processing of CNT/ZnO composites with controllable size, morphology and site [19].

As far as we know, the covalent link between functional groups (on the surface of CNTs) and foreign materials is favorable for the position-restricted modification of CNTs [20]. On the other hand, it has been demonstrated that single-walled carbon nanotubes (SWNTs) can be

*Corresponding author. Fax: +86 431 85168624.
E-mail address: jx_li@jlu.edu.cn (J. Li).

0022-4596/$ - see front matter © 2008 Elsevier Inc. All rights reserved.
doi:10.1016/j.jssc.2008.01.005

covalently modified by coupling amines (RNH_2), using carboxiimide chemistry to form amide linkages with carboxyl groups selectively [21]. For example, Sathyajith has synthesized the CNT–quantum dot (QD) heterojuctions with conjugation amine terminal groups (QD–NH_2) and acid-treated CNTs [22]. Single amine functionalized CdSe quantum dots were coupled to individual acid-chloride modified SWNTs by amide bond formation [23]. Herein, we report a simple wet-chemical route for the modification of MWNTs via zinc–ammonitum complex ion ($Zn(NH_3)_4^{2+}$) covalently attached to the MWNTs through the C–N bonds, by which both flower-like ZnO (FZ) on the tips of MWNTs and ZnO nanoparticles (ZNs) on the surface of MWNTs have been obtained, respectively, via adjusting the reaction time.

2. Experimental

A four-step method was employed in the preparation of MWNT/ZnO composites. Firstly, the MWNTs (commercial MWNTs) were treated with nitric acid (80%) at 80 °C for 4 h and washed with deionized water several times. A desired amount of $ZnCl_2$ (99%) were dissolved in deionized water. Then the $NH_3 \cdot H_2O$ solution was slowly added into the above solution under continuous stirring just when the white precipitate disappeared to form $Zn(NH_3)_4^{2+}$. Subsequently, the MWNTs were soaked into the solution for 30 min and 48 h at room temperature, respectively. The mass ratio of $ZnCl_2$ and MWNTs was 1:2. The soaking MWNTs were separated from the system centrifugally, and dried at 70 °C in vacuum. In this step, the intermediate products were obtained. At last, the intermediate products were calcined at 300 °C for 4 h at an atmosphere of nitrogen.

The products were characterized by scanning electron microscopy (SEM, JEOL JSM-6700F at 5 kV) and transmission electron microscopy (TEM, JEOL JEM 3010 at 300 kV) and X-ray diffraction (XRD, Rigaku XRD spectrometer with a Cu$K\alpha$ line of 1.54 Å). The infrared (IR) spectra were recorded on an IFS 66V/S FTIR spectrometer using KBr pellets. The photoluminescence (PL) properties of the MWNT/ZnO composites were measured at room temperature using a He–Cd laser operated at an excitation wavelength of 325 nm.

3. Results and discussion

Fig. 1a–c show the general morphology of the product soaked for 30 min. It can be obviously seen that a flower-like ZnO structure with a central petal and six radial petals growing from the center attaches on the tip of the MWNT to form a MWNT/flower-like ZnO heterojunction (MFZH). Most of the FZ structures are uniform with diameters from 600 nm to 1 μm and the surface of the flower is microscopically rough, but this rough surface consists of elongated particles rather than quasi-spherical ones. As shown in Fig. 1b, the angle between any two petals of flowers is about 60°, which should be due to the

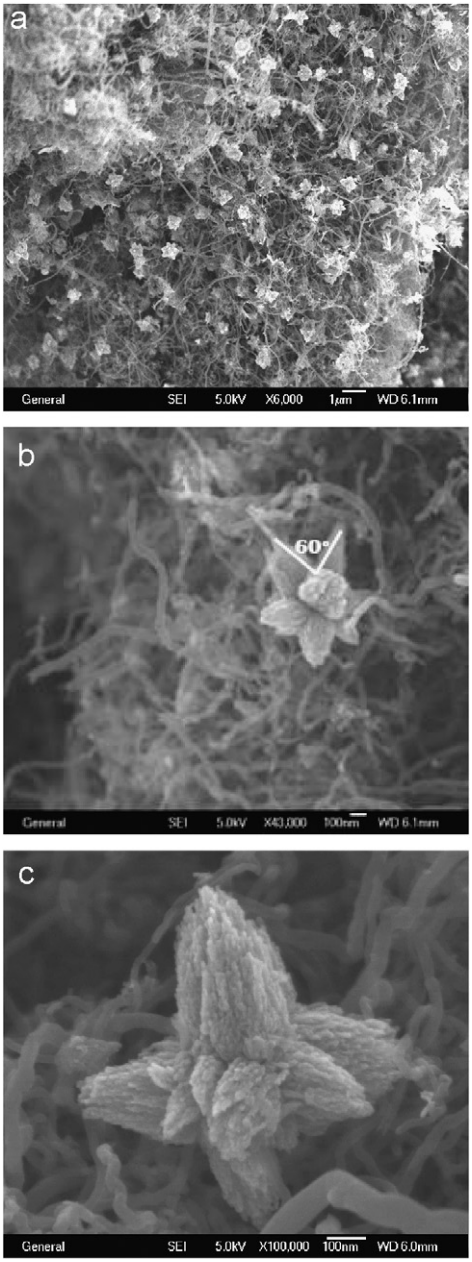

Fig. 1. (a–c) SEM images of the MFZHs.

crystal structure of ZnO [24]. It should be noted that a considerable amount of tips of the MWNTs do not get the FZ structures due to the small amount of as-synthesis ZnO. In our experiment, the mass ratio of $ZnCl_2$/MWNTs is 1:2, and the FZ structures are obtained. But further increase of the mass ratio of $ZnCl_2$/MWNTs results in the formation of bulk ZnO, and no FZ structures are present in the composite.

Further structural characterization of the heterojunction grown was performed by TEM. Fig. 2 shows the typical TEM images of the obtained MFZHs. It is obviously seen that FZ structures attach on the tips of the MWNTs which are in good agreement with the SEM images. The morphology of petals radially growing from the center also

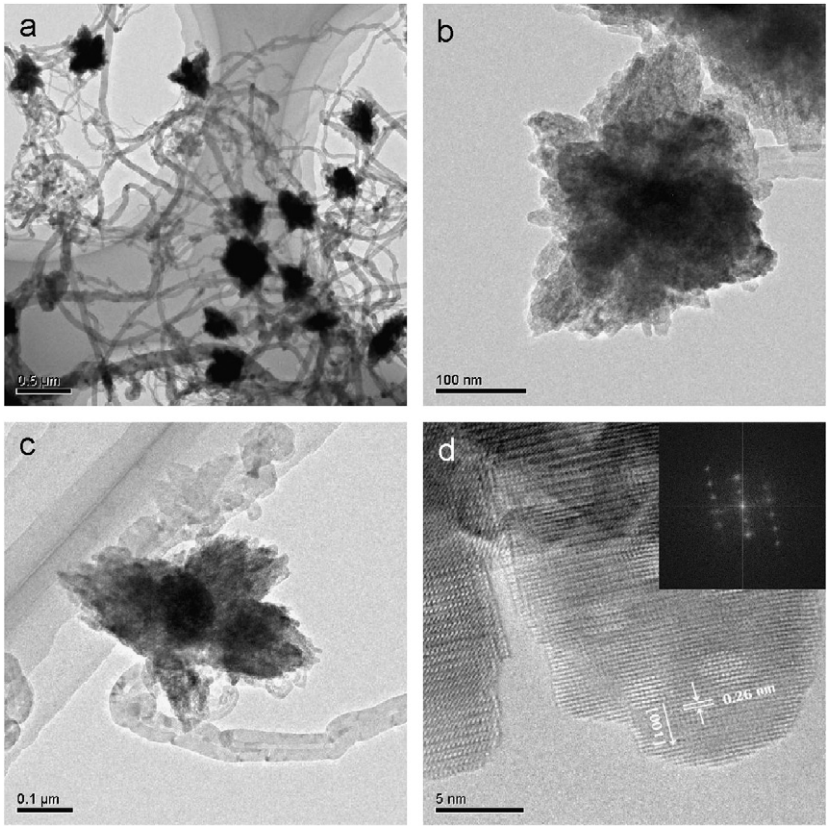

Fig. 2. (a–c) TEM images of the MFZHs. (d) The corresponding HRTEM of the petal of the flower-like ZnO structure. The inset is the Fourier transform of the HRTEM.

can be clearly seen. From the high-resolution (HR) TEM image recorded from the top of a petal of the FZ structure (Fig. 2d), the distance between the parallel lattice planes was measured to be 0.26 nm, which is coincident with the space between (0002) planes for wurtzite ZnO, confirming that the ZnO have wurtzite single crystalline structure grown along the [0001] *c*-axis direction. The Fourier transform of the image also confirms the growth direction of the petal being [0001] direction. It should be noted that some structural defects appear in the texture of the FZ. However, when the soaking time is prolonged to 48 h, the FZ structures disappear and are substituted by ZNs. As shown in Fig. 3a, it can be seen that a large-scale MWNTs are coated with ZnO nanoparticles to form MWNT/ZN composites (MZNCs). Fig. 3b shows more clearly quantum dots of ZnO coating on the surface of MWNTs densely. The corresponding HRTEM image in Fig. 3c demonstrates that ZnO nanoparticles are intimately connected to the MWNTs and the size of the ZnO nanoparticle is as small as about 5–10 nm.

The structures of the obtained products were further investigated by XRD. Fig. 4 demonstrates the XRD patterns of the pure MWNTs, MFZHs and MZNCs. It is clear that both MFZHs and MZNCs are mixture of two phases, including wurtzite ZnO and MWNT. All diffraction peaks of wurtzite ZnO can be readily indexed according to JCPDS file no. 36-1451, and the diffraction peak at $2\theta = 26.0^\circ$ and 44.4° can be assigned to (002) and (100) planes of MWNT or graphite, respectively.

Possible growth mechanism of MWNT/ZnO composites is schematically illustrated in Fig. 5. At first, acid treatment introduces the carboxyl groups (−COOH) into the MWNTs. Usually, the amount of carboxyl groups on the tips is more than that on the sidewalls of MWNTs because of the highest defect sites on the tips [22]. Secondly, when acid-treated MWNTs are soaked in the $Zn(NH_3)_4^{2+}$ solution at room temperature for 30 min, the concentration of the $Zn(NH_3)_4^{2+}$ on the tips of the MWNTs is rather high due to the presence of a large number of carboxyl groups. As a result, the concentration of $CONH–Zn(NH_3)_3^{2+}$ groups formed by the reaction of the amide and carboxyl in the intermediate products is high and favors the formation of flower-like structures on the tips of MWNTs after calcination. When prolonging the soaking time, the $Zn(NH_3)_4^{2+}$ are dispersed homogeneously around the MWNTs, and the concentration of $CONH–Zn(NH_3)_3^{2+}$ groups in the intermediate products is low and prefers the formation of nanoparticles around the MWNTs to that of flower-like structures on the tips after calcination. Generally, the formation of ZnO crystals involves two steps which are nucleation and growth, and the final morphology of crystals is partially determined by their intrinsic crystallographic structure [25]. At the initial stage, ZnO linked to MWNT is as droplets, and when the degree of

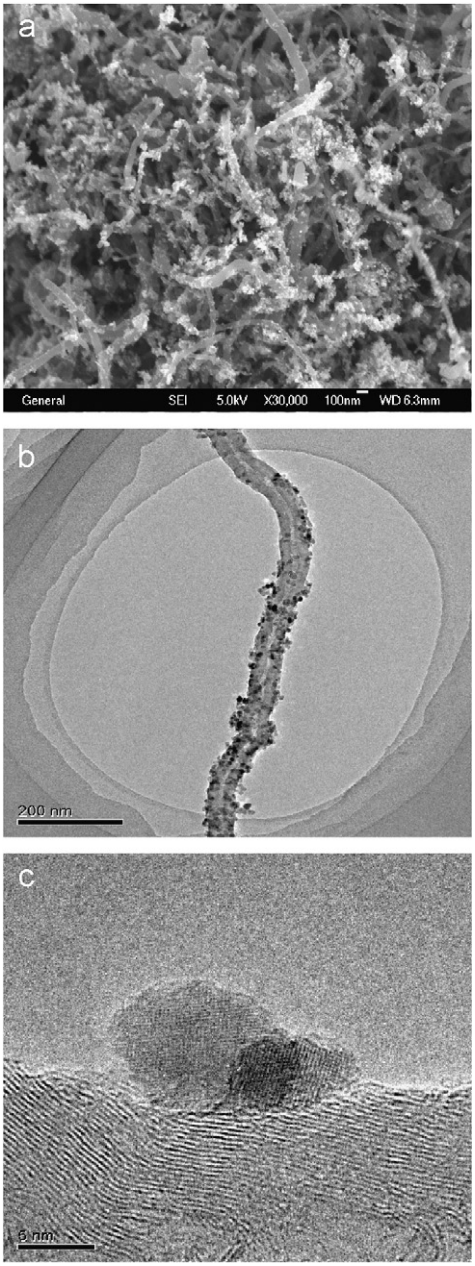

Fig. 3. (a) SEM image, (b) TEM image and (c) HRTEM image of the MZNCs.

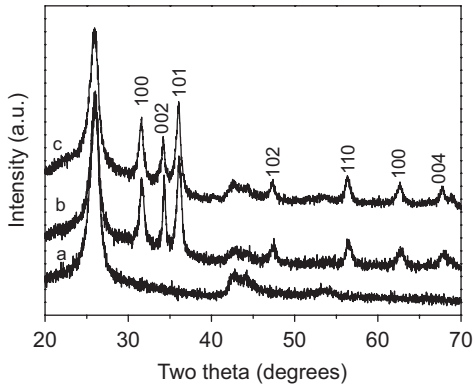

Fig. 4. XRD patterns of the (a) pure MWNTs, (b) MFZHs and (c) MZNCs.

super-saturation exceeded the critical value ZnO nuclei are naturally generated. In order to confirm this hypothesis, the products calcined for 1 h with the soaking time of 30 min was prepared (Fig. 6). It is clearly seen that ZnO crystals attach on the tips of the MWNTs and form MWNT/ZnO nanoparticle heterojunctions. After the formation of nuclei, the elongated ZnO particles can be formed around the circumference of ZnO nuclei due to the anisotropic growth to some extent. It has been reported that the formation of complex structure with radiating growth mode resulted from the growth of a central nucleus [26]. As illustrated in the SEM images, the ZnO flowers have six symmetrical branches around a longitudinal branch. This characteristic is strongly related to the crystal structure of ZnO nuclei. It is well known that ZnO has a basal polar oxygen plane ($0\,0\,0\,\bar{1}$), a top tetrahedron corner-exposed polar zinc plane (0001), and six low-index faces parallel to the [0001] orientation [24]. So the generated ZnO nuclei possess eight small facets and the theoretical and the most stable crystal habit is a hexagon elongated along the *c*-axis. The elongated ZnO particles provide active sites with *c*-axis preferred orientation for the further growth of petals in the FZ structures by a self-catalytic process [27].

For further confirming the feasibility of the mechanism mentioned above, we measured the IR spectra of the acid-treated MWNTs, intermediate product and MZNCs (Fig. 7). A band at 1720 cm^{-1} which is due to the stretch mode of carboxyl groups can be observed in the IR spectrum of the acid-treated MWNTs. This indicates that carboxylic acid groups formed on the surface of the MWNTs. The appearance of new bands in the range of 3400–3100 cm^{-1}, 900–650 cm^{-1} attributed to the N–H stretching vibration, and 1250–1000 cm^{-1} assigned to C–N stretching vibration in the IR spectrum of the intermediate product, gives an unambiguous evidence of the $Zn(NH_3)_4^{2+}$ attaching to the MWNTs. In the IR spectrum of MZNCs, the band at 469 cm^{-1} related to the Zn–O group and the band at 1720 cm^{-1} attributed to carboxyl groups which may be produced by the partially decomposition of the CONH–$Zn(NH_3)_3^{2+}$ groups in intermediate products were observed.

Room-temperature PL spectra of the MFZHs and MZNCs with an excitation wavelength at 325 nm are presented in Fig. 8. Both of them exhibit a broad green emission peak with maximum at 508 nm, which is known to be related to structural defects of ZnO crystals such as oxygen vacancies. And it is clear that the blue peak, associated with the recombination of free excitons in ZnO [28], shifts from 378 to 400 nm upon increasing the size of the ZnO nanostructures attached to the MWNTs. Such a red-shift with particle size is attributed to the quantum-confinement-induced enhancement of the energy gap [17]. Furthermore, it is worth noting that the intensity

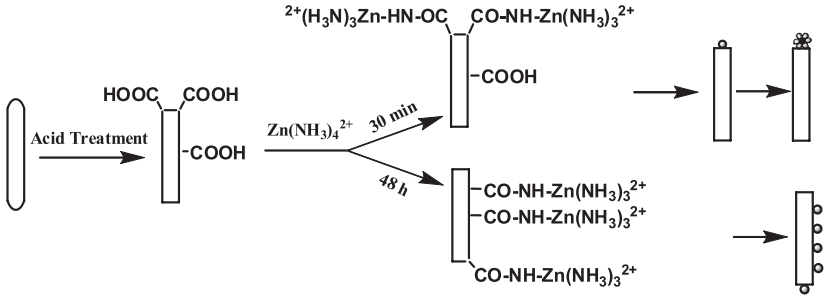

Fig. 5. Proposed growth mechanism of the MWNT/ZnO composites.

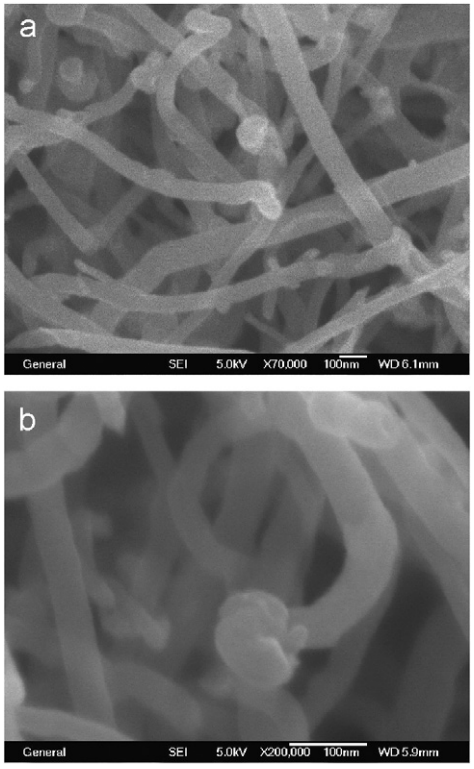

Fig. 6. SEM images of the sample calcined for 1 h with the soaking time of 30 min.

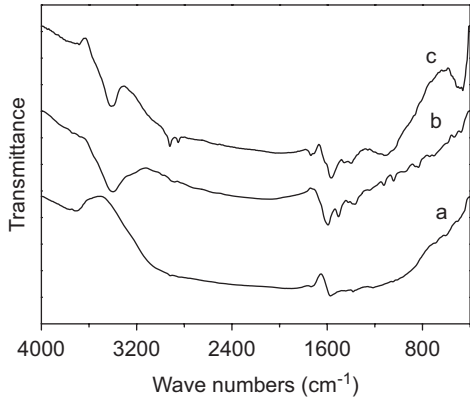

Fig. 7. IR spectra of the (a) acid-treated MWNTs, (b) intermediate product and (c) MZNCs.

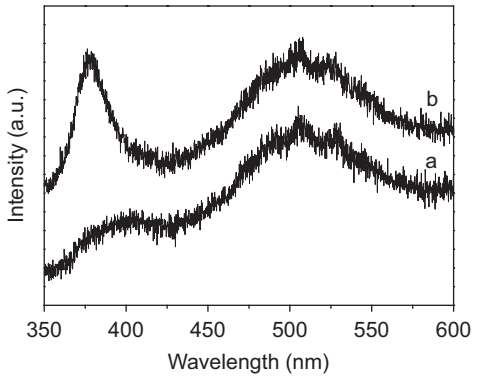

Fig. 8. PL spectra of the (a) MFZHs and (b) MZNCs.

ratio of the deep-level emission and the near-band-edge emission of the MZNCs is about 1:1, while that of the MFZHs is 2:1. It indicates that PL peak of ZNs directly attached to MWNTs is quenched to a considerable extent compared with that of FZ in the MFZHs. According to the former studies, it is due to the interaction of ZnO nanoparticles in excited state and MWNTs in electron transfer process [29].

4. Conclusion

In summary, a simple and effective method has been developed to modify MWNTs with ZnO nanostructures by zinc–ammonitum complex ion covalently attached to the MWNTs through the C–N bonds. The MFZHs and MZNCs could be obtained via adjusting the reaction time, respectively. The soaking time plays a key role in controlling the size, morphology, and site of the synthesized ZnO nanostructures attached to the MWNTs. PL measurements of the obtained products, strongly influenced by the ZnO nanostructures, have been performed. It is therefore that they are of great significance for the development of MWNT-based devices.

Acknowledgment

This work was supported by National Science Foundation of China under grant no. 10674054.

References

[1] S. Iijima, Nature 354 (1991) 56–58.
[2] H.Q. Cao, M.F. Zhu, Y.G. Li, J.H Liu, Z.Ni, Z.Y. Qin, J. Solid State Chem. (2007) doi:10.1016/j.jssc.2007.08.018.
[3] C.G. Zhao, L.J. Ji, H.J. Liu, G.J. Hu, S.M. Zhang, M.S. Yang, Z.Z. Yang, J. Solid State Chem. 177 (2004) 4394–4398.
[4] J. Kong, M.G. Chapline, H.J. Dai, Adv. Mater. 13 (2001) 1384–1386.
[5] S.E. Baker, W. Cai, T.L. Lasseter, K.P. Weidkamp, R.J. Hamers, Nano Lett. 2 (2002) 1413–1417.
[6] B.R. Azamian, J.J. Davis, K.S. Coleman, C.B. Bagshaw, M.L.H. Green, J. Am. Chem. Soc. 124 (2002) 12664–12665.
[7] V. Georgakilas, K. Kordatos, M. Prato, D.M. Guldi, M. Holzinger, A. Hirsch, J. Am. Chem. Soc. 124 (2002) 760–761.
[8] S. Banerjee, S.S. Wong, Nano Lett. 2 (2002) 195–200.
[9] W.Q. Han, A. Zettl, Nano Lett. 3 (2003) 681–683.
[10] S. Ravindran, K.N. Bozhilov, C.S. Ozkan, Carbon 42 (2004) 1537–1542.
[11] J.H. Shi, Y.J. Qin, W. Wu, X.L. Li, Z.X. Guo, D.B. Zhu, Carbon 42 (2004) 455–458.
[12] M.H. Huang, S. Mao, H. Feick, H. Yan, Y. Wu, H. Kind, E. Webber, R. Russo, P. Yang, Science 292 (2001) 1897–1899.
[13] W.I. Park, G.C. Yi, J.W. Kim, S.M. Park, Appl. Phys. Lett. 82 (2003) 4358–4360.
[14] H. Rensmo, K. Keis, H. Lindstrom, S. Sodergren, A. Solbrand, A. Hagfeldt, S.E. Lindquist, L.N. Wang, M. Muhammed, J. Phys. Chem. B 101 (1997) 2598–2601.
[15] S.M. Al-Hili, R.T. Al-Mofarji, M. Willander, Appl. Phys. Lett. 89 (2006) 173119-1–173119-3.
[16] J.W. Liu, X.J. Li, L.M. Dai, Adv. Mater. 18 (2006) 1740–1744.
[17] Y.W. Zhu, H.I. Elim, Y.L. Foo, T. Yu, Y.J. Liu, W. Ji, J.Y. Lee, Z.X. Shen, A.T.S. Wee, J.T.L. Thong, C.H. Sow, Adv. Mater. 18 (2006) 587–592.
[18] Y.P. Du, C.C. Hao, G.Z. Wang, Mater. Lett. (2007) doi:10.1016/j.matlet.2007.04.066.
[19] P. Jiang, J.J. Zhou, H.F. Fang, C.Y. Wang, Z.L. Wang, S.S. Xie, Adv. Funct. Mater. 17 (2007) 1303–1310.
[20] B.P. Jia, L. Gao, J. Phys. Chem. B 111 (2007) 5337–5343.
[21] S.S. Wong, A.T. Woolley, E. Joselevich, C.L. Cheung, C.M. Lieber, J. Am. Chem. Soc. 120 (1998) 8557–8558.
[22] S. Ravindran, S. Chaudhary, B. Colburn, M. Ozkan, C.S. Ozkan, Nano Lett. 3 (2003) 447–453.
[23] J.M. Haremza, M.A. Hahn, T.D. Krauss, Nano Lett. 2 (2002) 1253–1258.
[24] Z.L. Wang, J. Phys.: Condens. Matter 16 (2004) R829–R858.
[25] J. Zhang, L.D. Sun, H.Y. Pan, C.S. Liao, C.H. Yan, New J. Chem. 26 (2002) 33–34.
[26] H.S. Qian, S.H. Yu, J.Y. Gong, L.B. Luo, L.L. Wen, Cryst. Growth Des. 5 (2005) 935–939.
[27] Z.L. Wang, X.Y. Kong, J.M. Zuo, Phys. Rev. Lett. 91 (2003) 185502-1–185502-4.
[28] S.Y. Bae, H.W. Seo, H.C. Choi, J. Park, J. Park, J. Phys. Chem. B 108 (2004) 12318–12326.
[29] F. Vietmeyer, B. Seger, P.V. Kamat, Adv. Mater. 19 (2007) 2935–2940.